

Enhancement and quality control of GOES images

Marit Jentoft-Nilsen[†], K. Palaniappan[†], A. Frederick Hasler, Dennis Chesters

[†]Science Systems Applications Inc.

Laboratory for Atmospheres

NASA Goddard Space Flight Center, Greenbelt, MD 20771

Email: marit@camille.gsfc.nasa.gov, palani@camille, hasler@agnes, chesters@climate

ABSTRACT

The new generation of Geostationary Operational Environmental Satellites (GOES) have an Imager instrument with five multispectral bands of high spatial resolution, and very high dynamic range radiance measurements with 10-bit precision. A wide variety of environmental processes can be observed at unprecedented time scales using the new Imager instrument. Quality assurance and feedback to the GOES Project Office is performed using rapid animation at high magnification, examining differences between successive frames, and applying radiometric and geometric correction algorithms. Missing or corrupted scanline data occur unpredictably due to noise in the ground based receiving system. Smooth high resolution noise-free animations can be recovered using automatic techniques even from scanline *scratches* affecting more than 25% of the dataset. Radiometric correction using the local solar zenith angle was applied to the visible channel to compensate for time-of-day illumination variations to produce gain-compensated movies that appear well-lit from dawn to dusk and extend the interval of useful image observations by more than two hours. A timeseries of brightness histograms displays some subtle quality control problems in the GOES channels related to rebinning of the radiance measurements. The human visual system is sensitive to only about half of the measured 10-bit dynamic range in intensity variations, at a given point in a monochrome image. In order to effectively use the additional bits of precision and handle the high data rates new enhancement techniques and visualization tools were developed. We have implemented interactive image enhancement techniques to selectively emphasize different subranges of the 10-bits of intensity levels. Improving navigational accuracy using registration techniques and geometric correction of scanline interleaving errors is a more difficult problem that is currently being investigated.

Keywords: radiometric correction, histogram arrays, geometric registration, geostationary, GOES, satellite imaging

1. INTRODUCTION

A wide variety of atmospheric, land and ocean processes can be observed at unprecedented temporal and spatial resolution using the GOES Imager instrument. Examples of environmental and anthropogenic processes that we have observed over the past two years include rapid thunderstorm and front development, convective outbreaks along outflow boundaries, multilayer wind shear, evolution of hurricane cloud-top structure, microphysical properties of clouds, atmospheric gravity waves, Kelvin-Helmholtz and solitary waves in hurricane cloud structures, fog dissipation, plumes from shuttle launches, contrails from jet aircraft, snow deposition and evaporation, sun glint from clouds and water, urban heat islands, moon's shadow during solar eclipses, African and Amazonian dust storms, ash and heat from volcanic eruptions, smoke from forest fires and biomass burning, deforestation in Amazonia, atmospheric disturbances due to ship tracks, diurnal heating of land and water, river flooding and gyres in ocean currents¹.

The new generation of GOES have separate imaging and sounding instruments, additional spectral channels, improved spatial resolution, better spectral sensitivity, expanded number of quantization levels, a more accurate and stable sensor calibration, more precise pointing, navigation and registration accuracy, and adjustable scanning field of view². The new GOES are also three axes stabilized providing nearly continuous temporal coverage of the hemisphere. Some characteristics of the five channels of the GOES Imager instrument are shown in Table 1. The GOES Imager senses radiant (emitted) and solar-reflected energy in five channels from sampled areas of the Earth that provide spatial coverage from full-earth disk images to rapid scan continental USA (CONUS) and super-rapid scan sectors. Each sample (pixel) from the Imager is quantized to 10-bit accuracy linearly (versus 6-bits for GOES-7). A complete full earth image scan requires about 26.5 minutes and occurs every 3 hours and a sector scan covering 3000km × 3000km takes about 3 minutes to complete.

Channel No. (Wavelength)	Wavelength (μm)	Resolution (μrad)	IGFOV at Nadir (km) E/W x N/S	SSR (km) E/W x N/S
1 (visible, 0.65 μm)	0.52 to 0.72	28	1.0 x 1.0	0.57 x 1.0
2 (shortwave IR, 3.9 μm)	3.78 to 4.03	112	4.0 x 4.0	2.29 x 4.0
3 (water vapor, 6.7 μm)	6.47 to 7.02	224	8.0 x 8.0	2.29 x 4.0
4 (longwave IR, 10.7 μm)	10.20 to 11.20	112	4.0 x 4.0	2.29 x 4.0
5 (IR, 12.0 μm)	11.50 to 12.50	112	4.0 x 4.0	2.29 x 4.0

Table 1 GOES Imager characteristics including instantaneous geometric field of view (IGFOV), sampled subpoint resolution (SSR) which accounts for scanline oversampling by 1.75 for visible, 1.75 for IR window and 3.75 for H₂O band. The Imager data rate is about 2.6 Mb/s (1.2 GB/hour).

We have three main objectives in processing and enhancing GOES images. First, we want to identify and characterize problems with the images for quality assurance to provide feedback to the GOES Project Office at NASA Goddard Space Flight Center (GSFC), as this relates to satellite stability, instrument and ground sensor processing performance. Quality assurance consists of checking for and quantifying problems such as impulse or *salt and pepper* noise, scanline noise or *scratches*, line dropouts, scanline misregistration, detector striping, detector drift, stray light affecting detectors, radiometric bias, geometric distortion due to optics or spacecraft motion, all of which are readily apparent in multispectral images of single scenes. More subtle problems such as image jitter, small image misregistration and navigation errors can be found using timeseries animations of images. Second, we want to produce high quality science data of severe storms and mesoscale phenomena using automatic satellite data product generation such as stereo cloud heights³ and multispectral winds⁴ for numerical weather modeling. Third, we want to use timeseries animations and color enhancements of GOES data to qualitatively study weather patterns and provide World Wide Web Internet access to realtime full resolution datasets for public interest and education.

Many similar processing steps are used to meet these three objectives in processing a sequence of images. It requires that radiometric and geometric flaws be fixed so that the eye is not distracted from seeing more subtle details. Radiometric errors due to noise, light leakage, or detector scanning and performance have been well characterized for the new GOES Imager and automatic algorithms for correcting for most of these errors have been developed a few of which will be described in Section 2. Maintaining good cloud top detail from dawn to dusk for the visible channel is necessary for tracking a cloud's details during all stages of its formation and dissipation and extends the period over which visible data can be analyzed. Section 3 describes an automatic gain adjustment that compensates for the solar zenith angle and normalizes the albedo variation due to changes in illumination angle over the course of the day. For GOES Imager data it is also necessary to reduce the 10-bits of grayscale levels in the data to match the smaller range that can be more readily perceived by the human eye. Reducing the range of graylevel quantization within a GOES image usually destroys some of the perceivable fine scale structure, so techniques for enhancing the images before or during the grayscale requantization step is described in Section 4. Geometric errors caused by image jitter due to abrupt fixes in the GOES Image Navigation and Registration (INR) system or due to uncorrected spacecraft attitude changes can usually be corrected by applying advanced image registration techniques. However, as described in Section 5, local geometric distortion due to scanline shear from east-west or north-south interleaving errors is more difficult to correct.

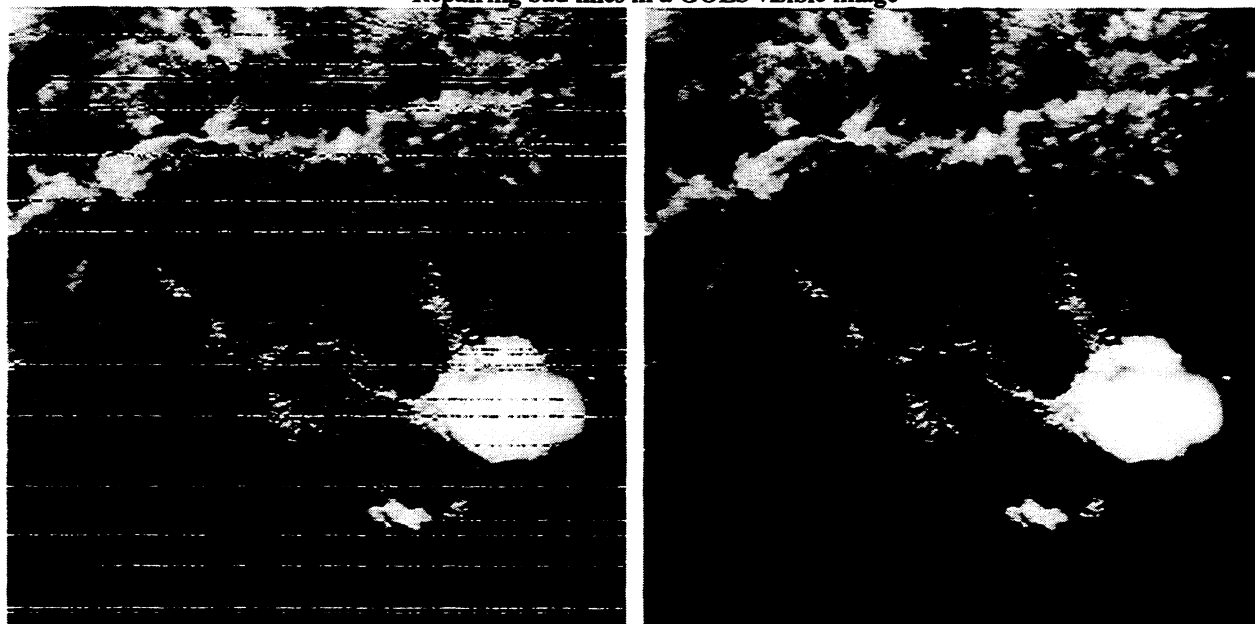
GOES-8 and GOES-9 each generate over 13 GB of data per day. It would be time consuming and inefficient to manually examine every Imager frame in detail, and the computing resources necessary to correct and archive all of the original as well as the corrected data generated by the quantitative quality control algorithms is prodigiously expensive. Furthermore, most of the quantitative algorithms that need to be applied, currently cannot keep up with the real-time data rate even when running on a fast supercomputer graphics workstation like the Silicon Graphics Inc. (SGI) Onyx with two R8000 (90 MHz) CPUs with a peak performance of 720 MFlops. Manually reviewing the output of these algorithms if they were run on every image is impractical without substantial resources. We use the following strategy to accomplish the three objectives described above in a cost effective manner. The Interactive Image Spreadsheet (IISS) developed in our laboratory is a powerful and versatile visualization software with a spreadsheet paradigm for handling large data volumes with high dynamic range measurements⁵. The IISS running on fast SGI workstations with large amounts of memory is used to view from several large to dozens or hundreds of smaller unenhanced GOES sectors from the realtime *ftp* server¹ singly or in animation. This allows us to find the most obvious quality control (QC) problems and observe the development of interesting weather situations. Then

semiautomatic processing software developed in our laboratory is run on the most interesting sector(s) of the day. The software fixes and enhances the images in the sector to produce an image animation suitable for further QC work or output to a NASA-TV video clip⁶. In the future, the GSFC GOES Web server is planned to have interactive sectorization and enhancement capabilities to provide data on demand from the rotating archive.

2. REPAIRING SCANLINE SCRATCH ERRORS IN GOES IMAGER DATA

Many of the missing and noisy GOES Imager scanlines are the result of bad reception at our antenna. Since the scanline scratches do not occur regularly within an image they cannot be readily identified and removed using Fourier transform methods. Figure 1a shows a GOES-9 visible scene from a series of 1-minute interval images with the noisy lines typical of bad reception at the NASA GSFC antenna. The scanline errors appear as horizontal *scratches* in the image and pose a challenge for creating smooth animations. Near the top of the image, there is also a line dropout (solid black line) of unknown origin. The noisy lines we see almost always occur singly, while the line dropouts often occur as gaps many lines wide. Software routines were written in the Interactive Data Language (IDL)⁷ to automatically recognize and replace these two types of bad lines.

Repairing bad lines in a GOES visible image



a. original image with bad lines

b. image with lines repaired by interpolation

Figure 1 (a) Original GOES-9 Imager picture (visible channel) of Florida from July 2, 1995 at 1844 UTC showing full and partial scanline scratches and dropouts. (b) The same image after application of automatic scanline repairing techniques.

Automatic average scanline radiance and correlation-based algorithms were developed to detect bad scanlines that extend most of the way across an image and interpolate across the noisy radiance measurements using spatially and temporally adjacent valid data. The line average,

$$\ell_{ave}(y) = \frac{1}{N_x} \sum_{x=0}^{N_x-1} I(x, y) \begin{cases} \geq T_\ell, & \text{normal scanline} \\ < T_\ell, & \text{corrupt scanline} \end{cases} \quad (2.1)$$

is thresholded to identify and flag bad lines; T_ℓ is a user-defined value, typically a fraction (e.g. 0.25) of the spacelook value in each channel. The scanline autocorrelation (each line's correlation to a copy of itself that has been shifted horizontally by one or more pixels) is computed for each scanline,

$$r(x, y) = \frac{1}{N_x} \sum_{m=0}^{N_x-1} I(m, y) I(x + m, y) \begin{cases} \geq T_a, & \text{normal scanline} \\ < T_a, & \text{corrupt scanline} \end{cases} \quad (2.2)$$

Scratchy scanlines are noisy and have low autocorrelation values, so scanline autocorrelations of lag one $r(1, y)$ that are less than the cutoff are used to detect corrupt scanlines. Both tests are needed since scanline dropouts which are nearly constant in value will have high autocorrelation values. The two tests can identify most of the bad lines, however, the two user-specified thresholds must be set differently depending on which of the five Imager channels is being processed. This technique does not work as well on visible Imager data near the terminator, because nighttime visible data, which is basically noise, is very uncorrelated.

Once a list of bad lines is generated, they are grouped into sets or gaps of adjacent bad lines and fixed in their entirety. For scanline gaps of one to three lines, the corrupt lines are replaced by interpolating between the previous and following good lines. Longer contiguous scanline gaps are replaced with data from a time-adjacent image. The data replacement is usually much less obvious in animation than when viewing a single image. When large gaps were repaired by interpolating between the previous and following time-adjacent images, the result was much more obvious and distracting in animations.

Figure 1a also shows several partially noisy lines that are only bad for a small fraction of the line. In order to minimize the amount of data replacement, a slightly different method is used to identify and replace partially scratchy scanlines. The absolute value of the difference between a line and its shifted copy is calculated and the differences are tested for segments with anomalous difference values to find sharp transitions.

$$\ell_{diff}(x, y) = |I(x, y) - I(x + 1, y)| \begin{cases} \geq T_d, \text{partially corrupt scanline} \\ < T_d, \text{normal scanline} \end{cases} \quad (2.3)$$

Segments of the line with bad values are marked in a mask for the whole image. After all the bad segments are found, each column is checked for bad pixels which are replaced with values interpolated between the preceding and following good pixels. The whole series of 1-minute GOES-9 images from which Figure 1a was taken had many noisy scanlines; in some scenes up to 25% of the image was corrupted. Repairing the images produced a satisfactory high-resolution animation and that could be used for testing automatic cloud tracking algorithms.⁸

3. SOLAR ILLUMINATION ANGLE CORRECTION

The GOES Imager visible channel measures reflected solar radiation. Figure 2 shows a histogram array for a day long GOES-9 series with each image of size 2444 x 1380 pixels, full resolution, and centered at (lat, lon) = (19.4°, -63.9°). The left histogram array, which is shaded to show highly populated bins in black and zero populated bins in white, shows the change in overall scene brightness as a function of time of day for raw images. When the scene is not illuminated (near 0900 UTC and 2330 UTC) the histogram distributions are centered on the spacelook count value with a very small spread. As the scene begins to be illuminated, the distributions begin to spread out and shift up in count space. At midday the process reverses and the range of counts diminishes until sunset. The two maxima in the histogram distributions, seen as dark regimes, are the maxima for land or water (low counts) and clouds (high counts). The two vertical stripes at 1545 UTC and 2030 UTC are due to very noisy data for these images.

The solar illumination angle correction assumes a Lambertian (diffuse) reflection model for the clouds being viewed and ignores any atmospheric effects between the clouds and the top of the atmosphere. In this simplified case, the reflected radiance from a scene, R , is the product of the scene albedo, ρ , the incident solar radiation, E , falling on the scene, and the cosine of the solar zenith angle,

$$R = \rho E \cos(z) \quad (3.1)$$

The equation converting GOES Imager counts X to radiance at the sensor is,

$$R = m(X - \text{spacelook}) \quad (3.2)$$

where m is a NOAA supplied calibration coefficient. This means that in count space, the sun illumination angle correction that converts measured counts to counts normalized to a sun zenith angle of zero is,

$$X' = \frac{(X - \text{spacelook})}{\cos(z)} + \text{spacelook} \quad (3.3)$$

For display purposes, we enforce the constraint that the cosine term in (3.3) needs to be greater than or equal to 0.1 in order to make the transition over the terminator smooth and to avoid dividing by zero in unilluminated parts of a scene.

The two solid black lines plotted on the left histogram array of Figure 2 are theoretical count values for $\rho = 0$ and $\rho = 1$ for the pixel in the scene with the maximum solar illumination. The lines were calculated using Equation 3.3 and the relationship, $\rho = cR$, where c is a NOAA supplied radiance to albedo conversion coefficient for converting $\text{mW}/(\text{m}^2 \text{ ster cm}^{-1})$ to albedo. The line for $\rho = 0$ is a flat line at the spacelook count value. The line for $\rho = 1$ is a curve that nearly coincides with the envelope of the histogram array. It is interesting to note, that there are a fair number of populated bins above the theoretical maximum count, especially at sunrise and sunset.

GOES-9 visible channel raw and sun angle corrected histograms

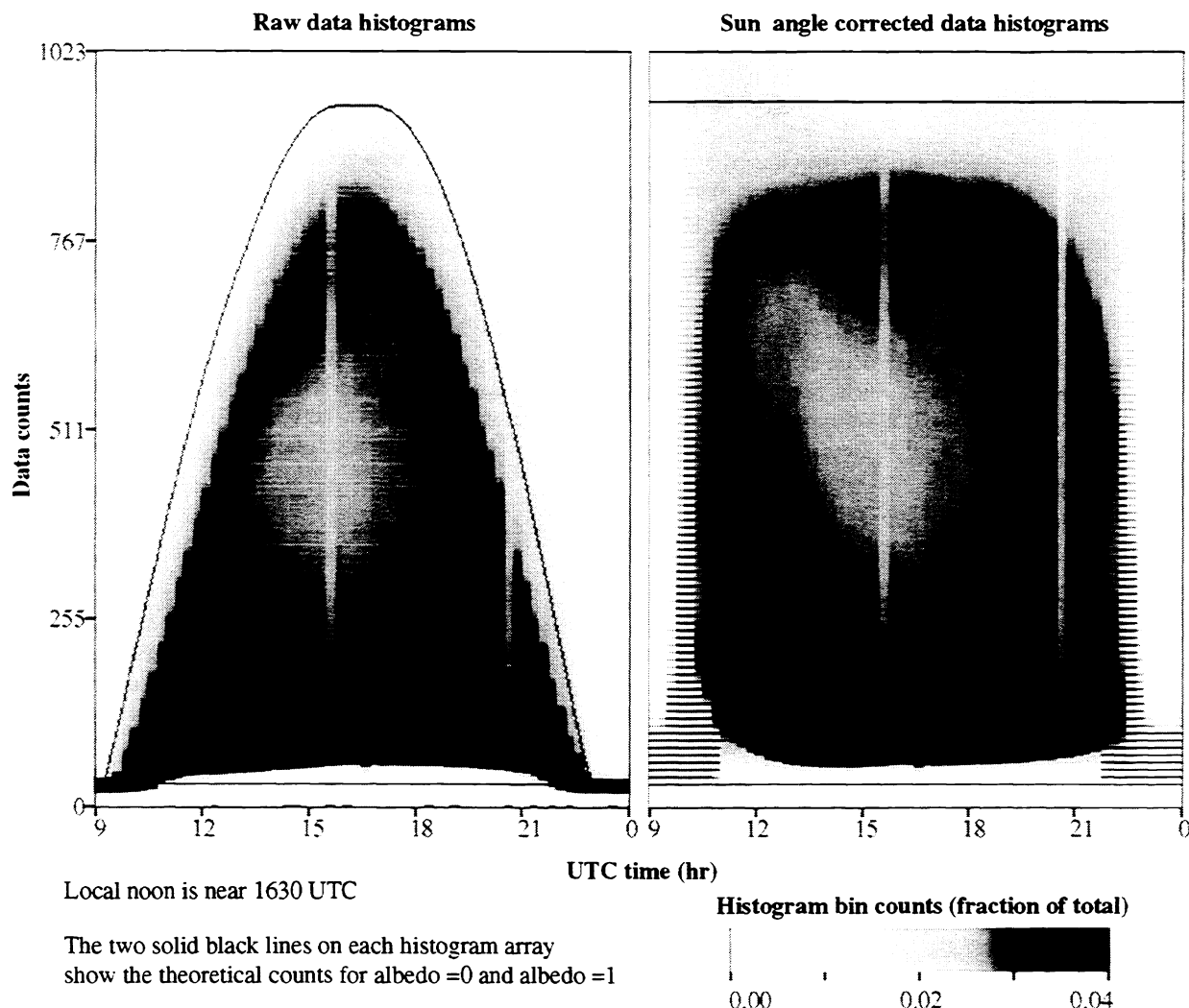


Figure 2 The left histogram array shows histograms for a day long series of GOES-9 Imager visible channel frames for scenes centered at (latitude, longitude) = (19.4°, -63.9°). The two solid black lines on each array show the theoretical count value for $\rho = 0$ and $\rho = 1$. The right histogram array is the result of applying the solar zenith angle correction.

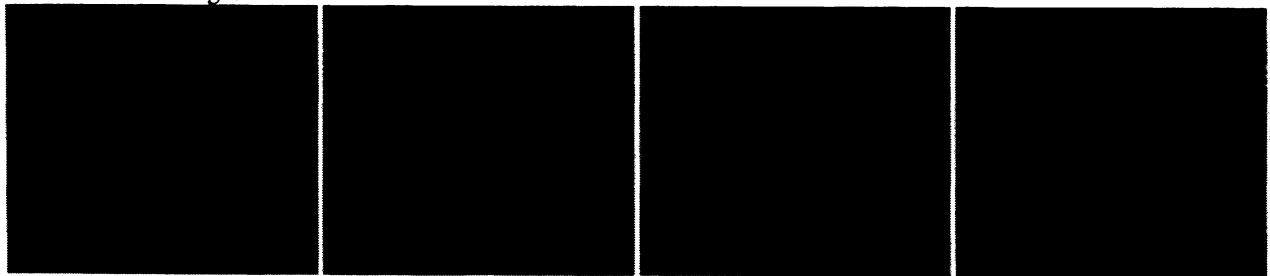
The histograms of the same images after the solar zenith angle correction has been applied are on the right half of Figure 2. As expected, the gray levels of the images are much more level over the course of a day after the correction, and the theoretical $\rho = 1$ line becomes a straight line because all the histograms have been normalized to the same amount of incident radiation. The clouds with apparent albedo greater than one are much more obvious in the corrected histogram array, and it is more evident that they occur most frequently for larger solar zenith angles. Some possible reasons why these clouds appear so bright are: they have higher altitudes and are illuminated longer than lower clouds or land, the lambertian reflection model is a

poor assumption for the clouds, that near sunrise and sunset the path in the atmosphere between the cloud top and top of atmosphere is longer so the amount of path scattered radiation is larger. The NOAA supplied radiance to albedo conversion factor is only an approximate conversion since the true albedo of any particular target would depend on all these factors listed.

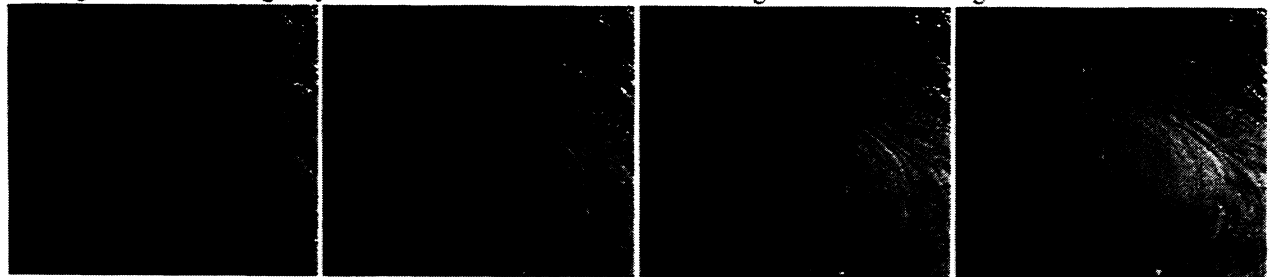
The automatic processing software uses the `xephem` program⁹ to calculate the subsolar point at the frame start time and then uses the solar zenith angle of the pixel closest to the subsolar point for the whole image. This is computationally much faster than calculating the zenith angle for every pixel in an image. For the images used to produce the histograms in Figure 2, calculating and applying the true correction for each pixel took 20 times longer (in IDL) than calculating the correction for one pixel and applying it to the whole image. The global approximation works well for scenes smaller than about 20 degrees of longitude. Figure 3 shows several raw and solar illumination angle corrected GOES-9 images of hurricane Luis.

Solar illumination angle correction of GOES-9 visible images

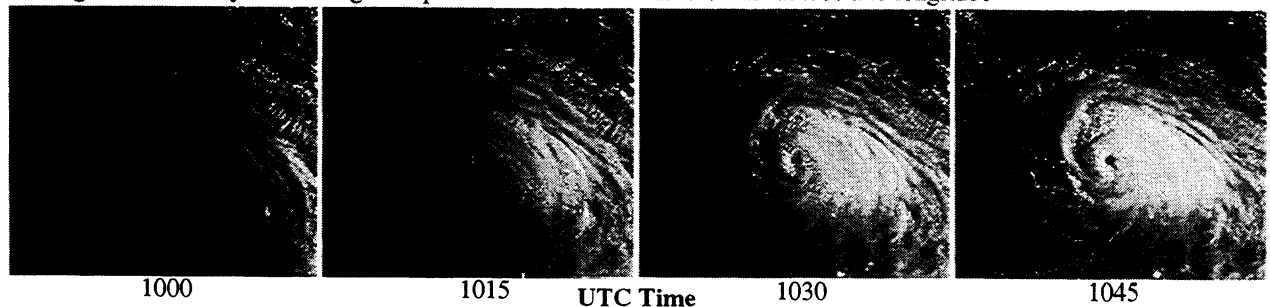
a. Uncorrected images



b. Images corrected using only the cosine factor of minimum zenith angle for the whole image



c. Images corrected by calculating each pixel's cosine factor based on its latitude and longitude



1000

1015

UTC Time

1030

1045

Figure 3 Results from two different techniques of solar illumination angle correction of GOES images from 6 Sep 95.

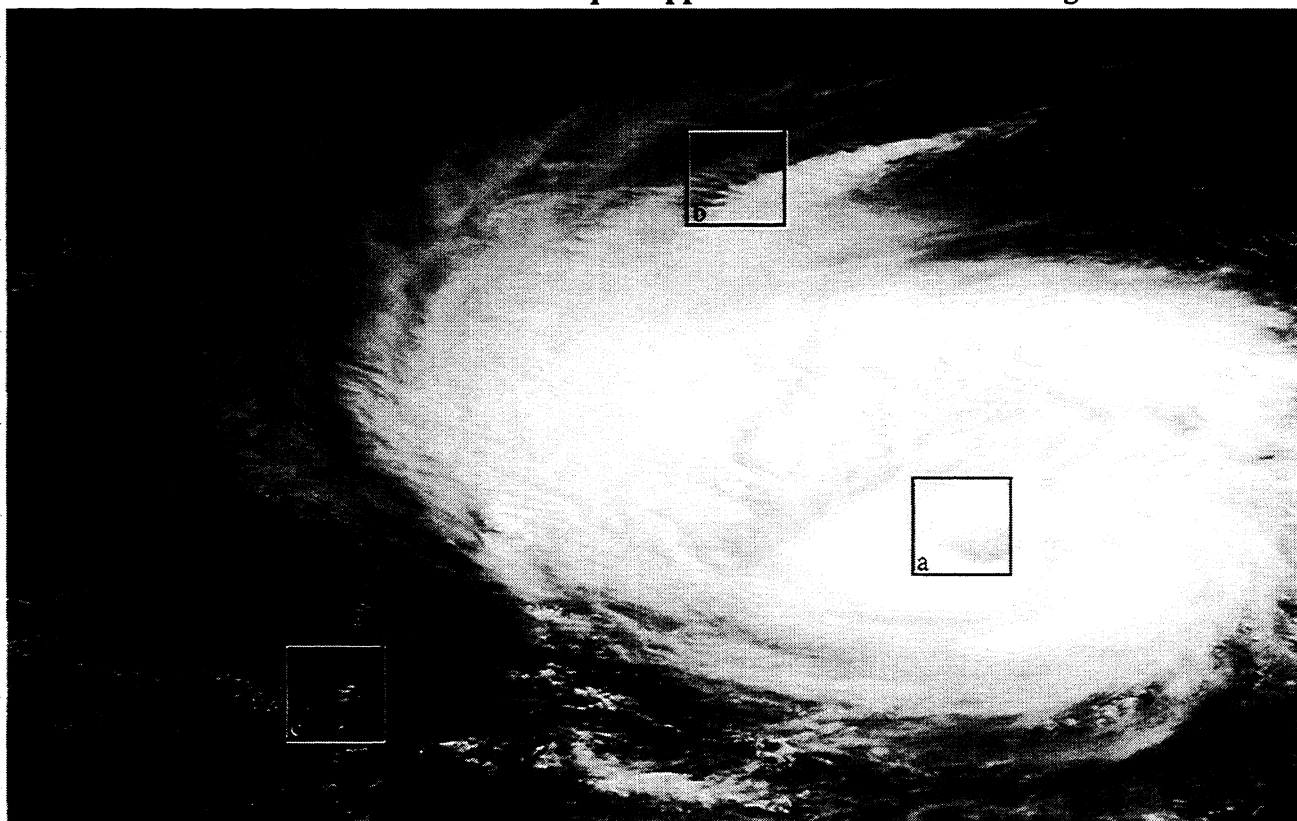
4. GRAY LEVEL QUANTIZATION AND IMAGE SHARPENING

The range of GOES multispectral Imager data is 10-bits or 1024 levels, which is wider than the limits of human perception for discriminating grayscale quantization levels. Figure 4 shows histogram arrays for a typical scene over a period of about 60 hours for each of the five GOES Imager channels from GOES-8. The visible channel has the largest range of gray levels, the 12 μ m and 11 μ m have slightly smaller min-max ranges, and the 3.9 μ m and 6.7 μ m channels have the smallest range.

Note that the histogram arrays are composed of a sequence of histograms with each individual scene histogram shown as a column of intensities in Figure 4. The effects of the daily solar illumination cycle can be seen not only in the visible channel (the gaps are during nighttime periods which would be seen as a black line), but also $3.9\text{ }\mu\text{m}$, $11\text{ }\mu\text{m}$ and $12\text{ }\mu\text{m}$ channels. The $3.9\text{ }\mu\text{m}$ channel saturates at the cold end during the nighttime; the detector clipping can be inferred from the sharp horizontal boundaries in the $3.9\text{ }\mu\text{m}$ histogram array. The $6.7\text{ }\mu\text{m}$ and $11\text{ }\mu\text{m}$ channels have distinct rebinning effects, which appear as holes in the respective histogram arrays, from processing done at NOAA before the data is rebroadcast in *gvar* format. All these features need to be considered when compressing the gray level counts to an appropriate range for human perception.

The human visual system is sensitive to only about 5-bits (32 levels) at a given point in a monochrome image which is half the 10-bit dynamic range in the Imager data. Additionally, most computer display monitors such as cathode ray tube (CRT) screens, liquid-crystal displays (LCD), plasma panels, or electroluminescent displays, as well as printed paper are capable of presenting even a smaller range of intensity levels (4 to 5-bits). We have tried several methods to enhance detail in GOES visible and IR images. The techniques we have used include contrast stretching, sharpening, unsharp masking, local and general histogram. Each of these methods has trade-offs in terms of computational speed, preservation of radiance information, stability over a timeseries of images, ability to enhance detail at all gray levels and amount of image dependent fine tuning of filtering parameters. In general it is not too hard to enhance a single GOES Imager channel using any of the techniques listed above to get informative and nice looking results. It is a little more difficult to enhance a timeseries of images for animation without introducing artifacts that cause distractions during the animation. Figure 5 shows a GOES-8 image of Hurricane Bertha showing subregions that were enhanced using different enhancement techniques. Corresponding animations will be available at <http://climate.gsfc.nasa.gov/~chesters/goesproject.html> and <http://rsd.gsfc.nasa.gov/rsd/movies/movies.html>.

Several enhancement techniques applied to a GOES8 visible image



Regions a,b and c are shown enhanced with several techniques in the second part of this figure

Figure 5a Visible GOES-8 image at 1 km resolution from 9 July 1996 showing three regions selected for enhancement.

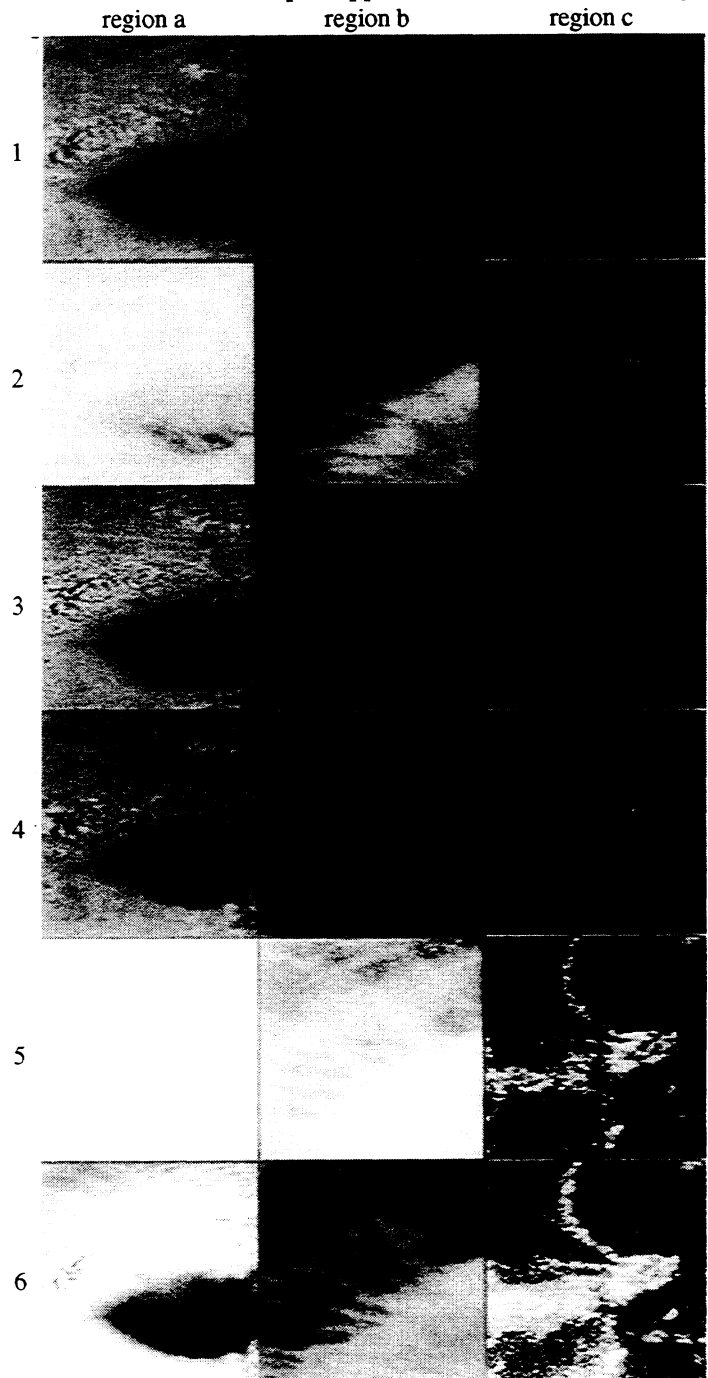
The simplest and fastest method of improving image contrast is to apply a lookup table that maps input data counts to the desired range of gray levels. If the mapping colormap lookup table mapping is monotonic, it is possible to calculate an approximate radiance for each rescaled gray level. Applying (colormap) lookup table transformations is stable for a timeseries of images and does not require any fine tuning to the particular image being enhanced. The main drawback with the lookup table approach is that it is not very good at compressing the number of gray levels in an image when there are details that need to be preserved throughout the quantization range. For GOES visible Imager data, it is possible to either enhance the cloud tops or to enhance the land and oceans. However, it is not possible to enhance both with a monotonic grayscale lookup table. Non-monotonic lookup tables can be used, but these lead to perceptual artifacts by adding structure to an image where the grayscale transformation mapping changes direction or has a discontinuity. The images available on the GOES public file server at GSFC-NASA¹ were all enhanced using lookup tables because it is fast and those downloading the images would then be able to calculate radiance from the gray levels. Figure 5a shows a GOES-8 visible image of Hurricane Bertha with three regions selected for enhancement. Figure 5b is divided into six rows, each showing the result of a different enhancement scheme. Row one in Fig. 5b shows the original image regions linearly stretched between minimum and maximum data counts, while Row 2 shows the same regions with a non-linear monotonic lookup table (i.e. square root transformation).

The second technique we use is convolution with a sharpening kernel such as

$$\begin{bmatrix} -1 & -1 & -1 \\ -1 & A & -1 \\ -1 & -1 & -1 \end{bmatrix} \quad (4.1)$$

High frequency emphasis by spatial filtering using small kernels is our current operational technique for the sector of the day because it is fast and it sharpens images without changing their low frequency characteristics. Figure 5b Row 3 shows an image that has been enhanced using the kernel in (4.1) with $A = 12$. Outlier pixels such as salt and pepper noise only effect their immediate neighborhood, so they do not produce large scale flickering in a timeseries of images. Radiance

Several enhancement techniques applied to a GOES8 visible image



- | | |
|--|----------------------------------|
| 1 - original image | 2 - nonlinear lookup table |
| 3 - convolution with sharpening kernel | 4 - unsharp mask |
| 5 - histogram equalization | 6 - local histogram equalization |

Figure 5b Images enhanced by applying six different graylevel enhancement techniques to the 3 regions shown in Fig. 5a to bring out cloud-top structure. Each technique incorporates graylevel quantization reduction to 8-bits.

values cannot be reliably retrieved from images processed with type of convolution.

Unsharp masking or high-boost filtering can also be implemented using a kernel similar to (4.1) but is usually done in two steps instead of one. The idea is to subtract a smoothed version of an image from itself. This is similar to applying a band stop filter to an image, where the stopped frequency corresponds to the size of the box used to create the smoothed version of the image. Correct radiance values cannot be retrieved from the data values in images enhanced this way. Unsharp masking is a moderately fast technique, but since the amount of enhancement depends on the input scene, it is sensitive to outlier pixels, noise or even general changes in image brightness. This is most evident in timeseries when using a medium-large box size for the smoothing step. For example, the appearance of a bright cloud can brighten nearby areas in the smoothed image whose brightness may not have changed in the original image. This will make the sharpened image darker in those areas. For a single image, this is not a problem, but it can cause flicker in a timeseries. The same effect causes 'ringing' around the edges in the sharpened image. One big advantage of unsharp masking as we use it (as a band stop to stop low frequencies) is that it enhances detail at all gray levels. The disadvantages are its moderate speed, the flicker mentioned about and the fact that it can need some tuning to the input data. Figure 5b Row 4 shows an image to which unsharp masking has been applied.

We have also tried various types of local and general histogram modification. General histogram equalization is the process of calculating and applying a lookup table to an image to make it have a flat (or any other shape) histogram. Histogram equalization is fast and preserves radiance values, but does have some problems when used to compress gray levels. One difficulty that arises for GOES Imager data is that the cloud top data counts are often in the tail at either end of the original histogram distribution. During the process of equalization, the original distribution tails are often mapped into a very small number of values in the output image, with the result that the cloud tops end up saturated. Figure 5b Row 5 shows an image that has been histogram equalized.

Local histogram modification is the same as general histogram equalization, except a histogram is calculated for a local area around each pixel in the input image and each pixel's value is adjusted according to its own histogram. This method enhances local detail better than the general histogram algorithm, but is much more computationally expensive. Also, depending on the size of the local area that is used to calculate the histograms, gray level shifts can occur in various parts of the output images making them unsuitable for animation. Figure 5b Row 6 shows an image that has been local histogram equalized.

Image enhancement for series of images involves some difficulties that are not present when processing a single image. For example, overall gray level changes from image to image in an animation can create a distracting flicker or strobing effect. When we enhance a series of images, we either have to avoid algorithms that effect the overall gray level or fine tune them to effect it consistently from image to image. This is a particular challenge for weather satellite images, since the scenes we are interested in can start out with large gray level changes in the form of clouds forming, dissipating and moving in and out of the scene. The changes in average gray level in the raw images are generally not distracting because they are caused by a bright object appearing against a constant or smoothly varying background.

5. GEOMETRIC DISTORTION DUE TO SCANLINE INTERLEAVING ERRORS

The new GOES satellite has improved navigational accuracy compared to GOES-7 including more precise pointing, navigation and registration accuracy using star sensing, landmark measurements, range from signal transmission time, compensation for orbit and attitude contributed image motion and compensation for scanning mirror or other instrument motion. The Image Navigation and Registration (INR) system operates in near real-time and was designed to meet stringent geographical location accuracy requirements.² However, adjacent scanlines in GOES Imager data are sometimes misplaced in either the north-south or east-west direction. Figure 6a shows east-west scanline shearing in a time series of several GOES-8 10.7 μm images. The shearing in this example shows up as two lines shifted several pixels to the east, as marked by the arrows. Figure 6b shows a similar situation with GOES-9 visible channel in a small island off the coast of the Dominican Republic. In this case, groups of 8 lines are shifted, causing the shape of the island and the coastline to the northeast to vary from image to image. Animating a time series of images at high magnification makes such shearing errors very obvious. We are currently investigating advanced registration techniques that may be useful for correcting such local geometric errors. Highly accurate navigation is needed for registering and matching images both in a time series for cloud tracking and in a stereo sequence from the two GOES satellites for stereo cloud heights⁴.

Scanline shear in GOES imager data

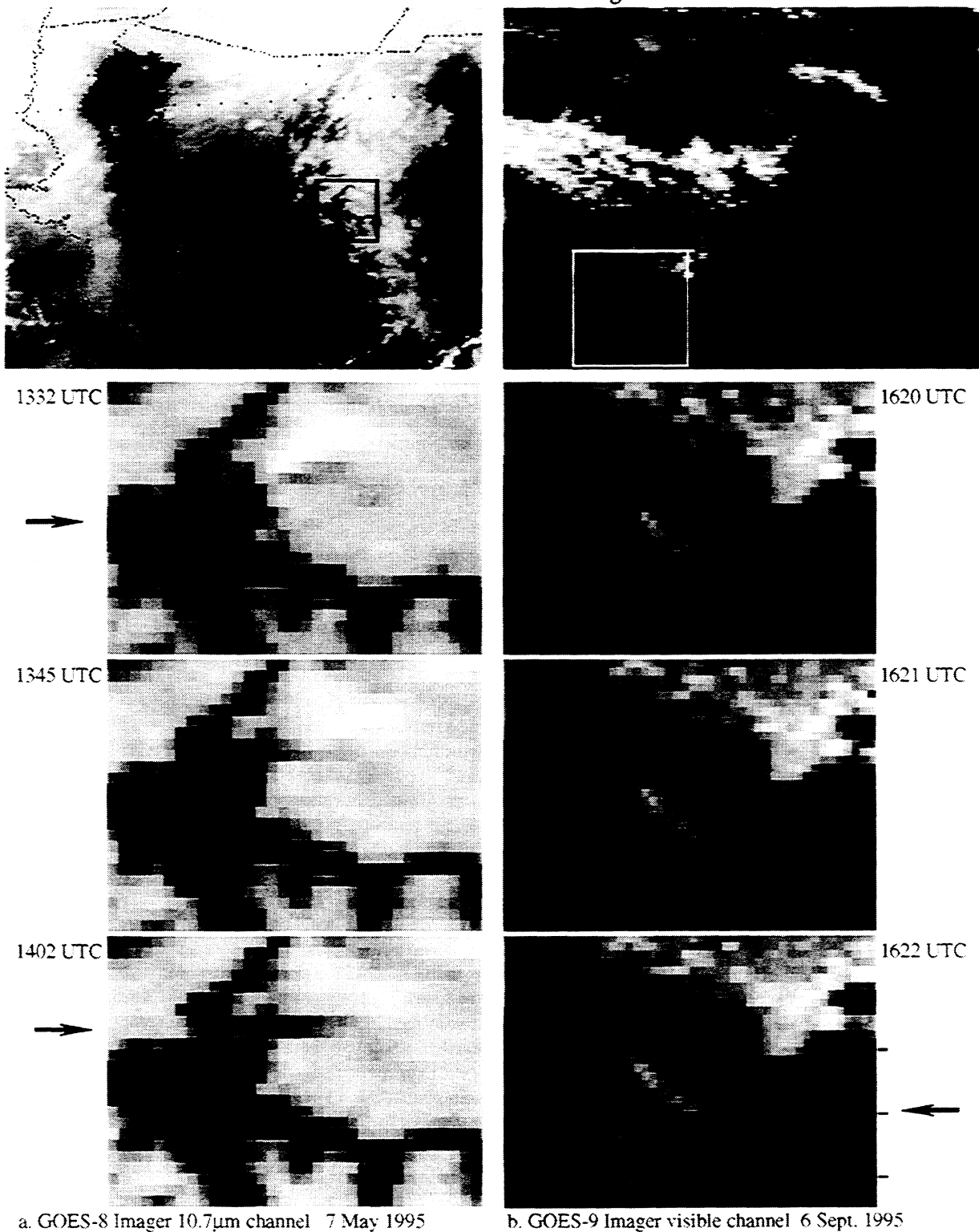


Figure 6 East-west scanline shear is evident in high contrast regions as shown in these (a) GOES-8 Imager scenes of the Sierra Madre mountains and (b) GOES-9 Imager scenes of Isla Beata off the coast of Dominican Republic.

6. CONCLUSIONS

A wide variety of atmospheric, land and ocean processes can be observed at unprecedented temporal and spatial resolution using the GOES Imager instrument. Smooth high resolution noise-free animations can be recovered using automatic techniques even from scanline *scratches* affecting more than 25% of the dataset. Radiometric correction using the local solar zenith angle was applied to the visible channel to compensate for time-of-day illumination variations to produce gain-compensated movies that appear well-lit from dawn to dusk and extend the interval of useful image observations by more than two hours. Image enhancement techniques and quantization methods for effectively using the full 10-bits of precision from the GOES Imager were developed.

7. ACKNOWLEDGMENT

This research was partially supported by the NASA RTOP 578-12-06-20, NASA AISRP program NRA-93-OSSA-09, NASA NRA-94-MTPE-02, NASA CAN-OA-94-01 and the NASA GSFC GOES Project Office.

8. REFERENCES

1. D. Chesters, O. Sharma, T. Nielsen, and A. F. Hasler, "GOES data ingest and public file service at NASA GSFC", *GOES-8 and Beyond*, SPIE Vol. 2812, Aug. 7-9, 1996 and <http://climate.gsfc.nasa.gov/~chesters/goesproject.html>.
2. W. P. Menzel and J. F. W. Purdom, "Introducing GOES-I: The first of a new generation of geostationary operational environmental satellites", *Bulletin of the American Meteorological Society*, Vol. 75, No. 5, pp. 757-781, May 1994.
3. K. Palaniappan, Y. Huang, X. Zhuang, and A. F. Hasler, "Robust stereo analysis", *IEEE Int. Symp. Comp. Vision*, IEEE Computer Society, Coral Gables, FL, pp. 175-181, Nov. 21-23, 1995.
4. K. Palaniappan, C. Kambhamettu, A. F. Hasler, and D. B. Goldgof, "Structure and semi-fluid motion analysis of stereoscopic satellite images for cloud tracking", *Int. Conf. Computer Vision*, IEEE Computer Society, Cambridge, MA, pp. 659-665, June 20-23, 1995.
5. A. F. Hasler, K. Palaniappan, M. Manyin, and J. Dodge, "A high performance Interactive Image SpreadSheet (IISS)", *Computers in Physics*, Vol. 8, No. 4, pp. 325-342, May/June 1994.
6. Peter Jennings, World News Tonight, ABC-TV Network, Hurricane Luis 1-minute GOES-9 animation sequence, Aired Sept. 6, 1995, 6:30 to 7:00pm.
7. Research Systems Inc., Interactive Data Language, Version 4.0.1, Boulder, CO.
8. K. Palaniappan, M. Faisal, C. Kambhamettu, A. F. Hasler, "Implementation of an automatic semi-fluid motion analysis algorithm on a massively parallel computer", *10th Int. Parallel Processing Symp.*, IEEE Computer Society, Honolulu, HI, pp. 864-872, April 15-19, 1996.
9. E. C. Downey, xephem program, C code available from <http://iraf.noao.edu/~ecdowney/xephem.html>, 1996.